Cardiac Image Segmentation Using Generalized Polynomial Chaos Expansion and Level Set Function

Yuncheng Du, Dongping Du, *Member, IEEE*

***Abstract*— Cardiovascular Magnetic Resonance (CMR) images involves a great amount of uncertainties. Such uncertainties may originate from either intrinsic measurement limitations or heterogeneities among patients. Without properly considering these uncertainties, image analysis may provide inaccurate estimations of cardiac functions, and ultimately lead to false diagnosis and inappropriate treatment strategy. In this work, a stochastic image segmentation algorithm is developed to separate cardiac chambers from the background of CMR images. To account for noise and uncertainties in pixel values, a generalized polynomial chaos (gPC) expansion is integrated with a level set function to dynamically evolve boundaries of cardiac chambers. Two consecutive steps are developed: a *deterministic segmentation* to identify an immediate neighborhood of boundary, of which pixel values are used to calibrate the gPC model; and a *stochastic segmentation* applied to the neighborhood region to evolve boundaries of cardiac chambers in a stochastic manner. The proposed method can provide a probabilistic description of the segmented heart boundary, which will greatly improve the reliability of image analysis, and potentially enhanced cardiac function evaluation.**

I. Introduction

Heart diseases cause more than 18 million deaths every year in the world [1]. Precise diagnosis of cardiovascular diseases and accurate evaluation of cardiac functions are essential for reducing cardiac mortality and improving cardiac care. Cardiovascular magnetic resonance (CMR) imaging has become an important technique in clinical cardiology practice because of its unique capability for non-invasive imaging of cardiac chambers and vessels [2]. CMR image analysis aims to provide detailed information on cardiac function, type and severity of heart disease, which can normally be inferred from such as the cardiac volume and ejection fraction. This requires to segment cardiac chambers from CMR images. However, due to the heterogeneities and variabilities among patients, CMR images involve uncertainty, and stochastic segmentation remains an open problem.

Uncertainty can significantly affect the accuracy of CMR image segmentation. The main idea of image segmentation is to identify the boundary of cardiac chambers and separate them from the background. Fig. 1 shows a typical image, where the blood pools in both right and left ventricles appear bright and their surrounding structures appear dark. CMR images (see image in Fig. 1) are stored as a multidimensional matrix, in which each element is defined as a pixel value [2, 3]. Image segmentation is to delineate the cardiac chambers by clustering pixel values. It should be noted that images can be corrupted by noise and uncertainty resulting from either measurement limitations or heterogeneities among patients.

Any uncertainty in pixel values may result in different segmentation results, e.g., the boundary of left ventricle (LV) in Fig. 1, is blurry due to non-compact myocardium. Different image segmentation techniques to find LV boundary will lead to different heart models. Without properly considering these uncertainties (e.g., non-compact myocardium), image analysis may provide inaccurate estimations of cardiac parameters, and ultimately lead to false diagnosis and inappropriate treatment strategy. Uncertainty quantification in CMR images analysis has been studied in the literature [2]. Previous works describe pixel values as probability distributions, which results in the notion of stochastic images [4, 5, 6]. However, most of the works require the calibration of a segmentation model. The performance of such a model greatly rely on the density of data used for calibration. In this work, we propose to quantify and propagate uncertainty in each CMR image using a generalized polynomial chaos (gPC) expansion [7].

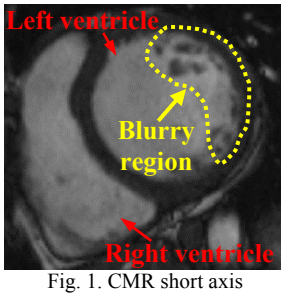

Fig. 1. CMR short axis view of heart

Our method integrates a gPC model with the *active contour without edges* method [8] to differentiate cardiac chambers from the background of images. The key idea is to evolve the boundary of cardiac chambers with a probabilistic description, which can be represented using a gPC approximation. This is then combined with level set function in the *active contour without edges* method. Rather than a fixed boundary, this combination can offer a probabilistic description of the boundary, thus the segmentation result is more reliable.

The rest of the paper is organized as follows: Section II gives a brief review of *active contour without edges* method and details the research methodology, i.e., generalized polynomial chaos (gPC) expansion-based stochastic image segmentation. Experimental results and discussion are given in Section III, which is followed by Conclusions in Section IV.

II. Stochastic Image Segmentation

A. Active Contours without Edges

The active contours method evolves a curve to estimate the boundary in an image U_0, and identifies objects from image's background. Define the curve as C, subjected to constraints of a given image in an open bounded domain Ω of R^2, which approximates the boundary φ, i.e., $C \approx \varphi$, $C \subset \Omega$, and $\varphi \subset \Omega$. To solve C, active contours [8, 9] finds a best estimate of C by

This work was supported by the National Science Foundation (CMMI – 1646664)

Y. Du is with the Department of Chemical and Biomolecular Engineering, Clarkson University, Potsdam, NY 13699 USA (e-mail: ydu@clarkson.edu).

D. Du is with the Department of Industrial, Manufacturing, and Systems Engineering, Texas Tech University, Lubbock, TX 79424 USA (phone: 806-834-7388; fax: 806-742-3411; e-mail: dongping.du@ttu.edu).

minimizing an energy function as:

$$\begin{aligned}\arg\min_{m_1,m_2,C} \quad & \mu_1 \cdot Length\,(C) + \mu_2 \cdot Area\,(inside\,(C)) \\ & + \lambda_1 \int_{inside(C)} \left|U_0(x,y) - m_1(C)\right|^2 dxdy \\ & + \lambda_2 \int_{outside(C)} \left|U_0(x,y) - m_2(C)\right|^2 dxdy\end{aligned} \tag{1}$$

, where μ_1, μ_2, λ_1 and λ_2 are parameters, m_1 and m_2 are the mean values of pixel values inside and outside C, respectively. x and y define the coordinates of a pixel value in Ω.

The optimization in (1) is solved with a level set function [8, 9], where C is replaced by an unknown level set function Z. Instead of manipulating C, the optimization in (1) is to find a geometric locus of a zero level set function Z. In this way, optimization in (1) is rewritten as:

$$\begin{aligned}\arg\min_{m_1,m_2,C} \quad & \mu_1 \cdot \int_\Omega \delta_\varepsilon(Z(x,y)) \left|\nabla Z(x,y)\right|^2 dxdy \\ & + \mu_2 \cdot \int_\Omega H_\varepsilon(Z(x,y))\, dxdy \\ & + \lambda_1 \int_\Omega \left|U_0(x,y) - m_1\right|^2 H_\varepsilon(Z(x,y)) dxdy \\ & + \lambda_2 \int_\Omega \left|U_0(x,y) - m_2\right|^2 (1 - H_\varepsilon(Z(x,y))) dxdy\end{aligned} \tag{2}$$

, where H_ε means a Heaviside function *w.r.t.* Z, and δ_ε is a regularized Dirac δ-function calculated with the derivative of H_ε [8]. The minimization of (2) is solved by updating m_1, m_2 and Z alternatingly.

For a fixed Z, values of m_1 and m_2 are means of pixel values inside and outside the zero level set function Z. For fixed m_1 and m_2 values, a gradient descent method can be formulated for Z *w.r.t.* an artificial time t as:

$$\begin{aligned}\frac{\partial Z}{\partial t} = \delta_\varepsilon(Z)[\mu_1 \cdot div\left(\frac{\nabla Z}{|\nabla Z|}\right) - \mu_2 \\ - \lambda_1 (U_0 - m_1(Z))^2 + \lambda_2 (U_0 - m_2(Z))^2]\end{aligned} \tag{3}$$

$$Z(0,x,y) = Z_0(x,y) \quad in\ \ \Omega \tag{4}$$

$$\frac{\delta_\varepsilon(Z)}{|\nabla Z|}\frac{\partial Z}{\partial \vec{e}} = 0 \qquad on\ \ \partial\Omega \tag{5}$$

, where $\vec{e}$ is the outward normal to the boundary $\partial\Omega$. Then, the optimization of (3) can be solved by recursive iterations [9]. To preserve the regularity of Z, a level set regularization term can be used [10], which ensures the stability. The minimum of (3) is solved by optimizing the energy function as:

$$\begin{aligned}\frac{\partial Z}{\partial t} = \delta_\varepsilon(Z)[\mu_1 \cdot div\left(\frac{\nabla Z}{|\nabla Z|}\right) - \mu_2 \\ - \lambda_1 (U_0 - m_1(Z))^2 + \lambda_2 (U_0 - m_2(Z))^2] + r(Z_t)\end{aligned} \tag{6}$$

The optimization (6) can be solved by a semi-implicit gradient descent algorithm [8, 9].

B. Generalized Polynomial Chaos Expansion

In this work, pixel values are described as random variables to account for uncertainties in a CMR image. The generalized polynomial chaos (gPC) expansion [6] is used to approximate pixel values with a finite second order moment as:

$$U(\omega) = \sum_{i=1}^{\infty} u_i \Phi_i(\xi(\omega)) \tag{7}$$

, where U is pixel values of a CMR image, $\xi = \{\xi_1, \ldots, \xi_n\}$ is a set of independent, identically distributed random variables from Wiener-Askey frame with a prior known probability density functions (PDFs) defined by random events ω. The $\Phi_i(\xi)$ are multi-dimensional orthogonal basis functions of ξ. u_i denotes the gPC coefficients. To reduce computational cost, (7) is truncated into a finite number of terms as:

$$U(\omega) \approx \sum_{i=0}^{p} u_i \Phi_i(\xi(\omega)) \tag{8}$$

, where p is the total number of terms used to represent a prior known distribution of pixel values of a CMR image U.

For simplicity, suppose that the evolving level set function Z at each artificial time instant t is defined as:

$$Z_t = f(U_0, t, Z_0) \tag{9}$$

, where f is an operator representing the image segmentation algorithm, i.e., (6), U_0 is a grayscale image to be segmented, and Z_0 defines an initial level set function.

To form a stochastic image segmentation algorithm, pixels values are approximated with (8). To quantify the effect of uncertainty on the evolution of the zero level set function Z, a gPC approximation of Z at each time interval t is defined as:

$$Z_t(\omega) \approx \sum_{i=0}^{P} \zeta_i \Phi_i(\xi(\omega)) \tag{10}$$

, where ζ_i are the gPC coefficients used to describe Z at time t. P is the total number of terms used to approximate Z, and is defined in (11) below. It is a function of polynomial degree p and the total number of random variables $\xi = \{\xi_1, \ldots, \xi_n\}$.

$$P = ((p+n)!/(p!n!)) - 1 \tag{11}$$

Substituting the gPC expansions of the level set function Z in (10) into the segmentation model, (9) is rewritten as:

$$\begin{aligned}& Z_t(\omega) \approx f(U(\omega), t, Z_0(\omega)) \\ & \sum_{i=0}^{P} \zeta_i \Phi_i(\xi(\omega)) \approx f\left(\sum_{i=0}^{p} \alpha_i \Phi_i(\xi(\omega)), t, \sum_{i=0}^{P} \zeta_{0,i} \Phi_i(\xi(\omega))\right)\end{aligned} \tag{12}$$

, where $\{\zeta_{0,i}\}$ are the gPC coefficients of an initially level set function. Using the Galerkin projection, the gPC coefficients in (10) are calculated by projecting (12) onto each of the polynomial chaos basis functions $\Phi_i(\xi)$ as:

$$\left\langle Z_t(\omega), \Phi_i(\xi) \right\rangle = \left\langle f(U(\omega), t, Z_0(\omega)), \Phi_i(\xi) \right\rangle \tag{13}$$

, where '$\langle\cdot,\cdot\rangle$' denotes an inner product between two vectors defined as follows:

$$\left\langle \psi_1, \psi_2 \right\rangle = \int \psi_1 \psi_2 \varpi(\xi) d\xi \tag{14}$$

, where the integration is calculated over a domain generated by ξ. $\varpi(\xi)$ is a weighting function and is selected *w.r.t.* the polynomial basis functions used to represent ξ so as the result in (14) is either 0 or 1. Polynomial basis functions are selected to satisfy the orthogonality in the Wiener-Askey scheme [6].

Once the gPC coefficients in (8) are available, it is possible to calculate the gPC coefficients of Z at any time t with (12) to (14). The mean and variance of the level set function Z can

be easily computed with gPC coefficients [6, 7]. This enables a quick calculation of statistical moments of Z_t. For example, the variance of the zero level set function values Z provides probability distributions along the segmentation boundary.

C. Stochastic Level Set Function based Segmentation

Suppose pixel values are described by random variables ξ, the stochastic level set function based segmentation is derived by replacing all variables in (6) with their corresponding gPC approximates. For stochastic image segmentation, the level set function Z can be formulated following the steps described in the previous section as a function of random variables ξ and polynomial basis function $\Phi_i(\xi)$. Substituting (8) and (10) into (6), the stochastic segmentation algorithm is formed as:

$$\frac{\partial Z(\xi)}{\partial t} = \delta_\varepsilon(Z(\xi))[\mu_1 \cdot div\left(\frac{\nabla Z(\xi)}{|\nabla Z(\xi)|}\right) - \mu_2 - \lambda_1(U(\xi) - m_1(Z(\xi)))^2 + \lambda_1(U(\xi) - m_2(Z(\xi)))^2] + r(Z(\xi)) \quad (15)$$

, where $Z(\xi)$ is estimated with (10), $m_1(Z(\xi))$ and $m_2(Z(\xi))$ are mean values inside and outside the geometric locus of a zero let set function, i.e., mean value of gPC estimations in (10). $\delta_\varepsilon(Z(\xi))$ is the derivative of a stochastic Heaviside function.

As seen in (15), Z is a function of random variables ξ that are used to represent pixel values with a gPC model in (8). The mean of pixel values of segmented regions, i.e., cardiac chambers $m_1(Z(\xi))$ and background $m_2(Z(\xi))$, are stochastic quantities calculated with (8). It is worth mentioning that only the mean values from the gPC models are used in this work.

The key idea in this work is the efficient approximation of pixel values with a gPC model. The PDF of pixel values can be calibrated with part of imaging data. However, this is less efficient since each image has different pixel values resulting from heterogeneity in patients. To calibrate the PDF of pixel values in each CMR image, a two-step image segmentation is developed: (*i*) a *deterministic segmentation* using the active contour method to identify the boundary of cardiac regions, and (*ii*) a *stochastic segmentation* applied to the immediate neighborhood along the boundary.

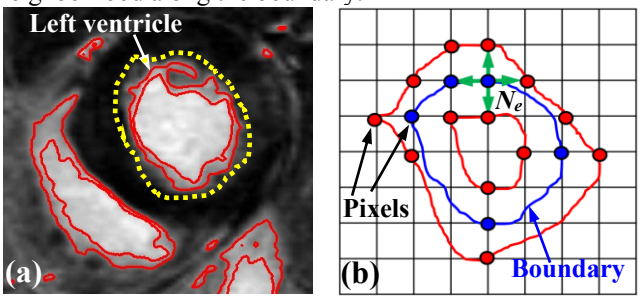

Fig. 2. Schematic of immediate neighborhood along the boundary

As seen in Fig. 2-a, two curves (in red) in the circled region represents the immediate neighborhood of the left ventricle. This is generated as follows: (*i*) Set a value N_e as shown in Fig. 2-b that is a number of pixels in the neighborhood of each pixel along the boundary (blue line) estimated with the *deterministic segmentation*; (*ii*) Connect pixels around the boundary to build an immediate neighborhood (enclosed area with red lines). The mean and variance of pixel values in the immediate neighborhood are used to calibrate a gPC model in (8). In this way, the gPC model is adjusted for each individual neighborhood in an image. For the calibration purpose, it is assumed for simplicity that pixel values in the neighborhood depend on only one random variable, i.e., ξ_1. Thus, the mean and variance of pixel values are calibrated as:

$$\min_{\kappa} J = \sum_{i=1}^{n}(\vartheta_{1,i} - \upsilon_{1,i})^2 + \sum_{i=1}^{n}(\vartheta_{2,i} - \upsilon_{2,i})^2 \quad (16)$$

, where the decision variables κ are the means and variances of pixel values in the neighborhood, $\vartheta_{1,i}$ and $\vartheta_{2,i}$ are the mean and variance that are estimated with a gPC model. The terms $\upsilon_{1,i}$ and $\upsilon_{2,i}$ are the mean and variance of the pixel values that are numerically calculated with pixels found to be inside the neighborhood estimated with the *deterministic segmentation*.

To summarize, the proposed two-step image segmentation involves initialization, model calibration, and segmentation. It should be noted that the stochastic formation of (15) and the calibration of (16) can be solved with a Monte Carlo (MC) simulations-based techniques. However, based on our studies [11] that compared gPC vs. MC, the computational effort with MC is significantly higher.

III. Results and Discussion

A. Uncertainty quantification and gPC model calibration

The accuracy of stochastic image segmentation depends on the gPC model of pixel values. This relies on the polynomial basis functions and the number of terms used in (8). The basis function should be appropriately selected with the statistical distribution of pixel values in neighborhoods while ensuring the orthogonality. Fig. 3 shows segmentation results using the deterministic algorithm and the PDFs of pixel values in neighborhoods generated when N_e is 1.

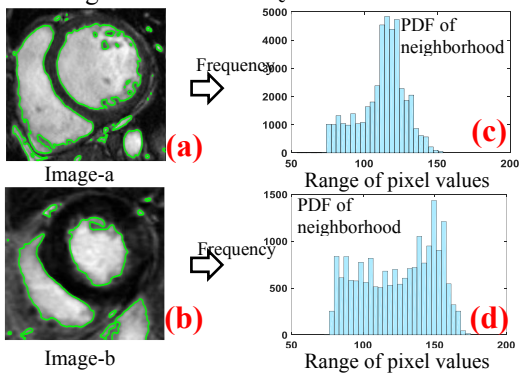

Fig. 3. Illustration of segmentation and PDF profiles of pixel values

As seen in Fig. 3, the green lines describe the boundary that separates the cardiac regions from the image background. The boundary corresponds to pixels where $Z \approx 0$. It should be noted that segmentation algorithms segment left and right ventricles from the background simultaneously. Since the left ventricle appears as a circular region, a special mathematical treatment to estimate shape information, i.e., center point and radius of a circle, is used to discern left ventricle from right ventricle. However, details are not discussed in this work for brevity.

For clarification, the PDF profile of the pixel values in the neighborhood regions of left ventricles is approximated using a binning algorithm (See Fig. 3 c & d). As shown in Fig. 3-c and 3-d, pixel values in each neighborhood of left ventricle have different distributions that are not standard distributions in the Wiener-Askey scheme. To quantify the PDFs, meanwhile, ensure the orthogonality and reduce the number of terms used in (8), the Gram-Schmidt polynomials [12] are used as basis functions to capture stochasticity in pixel values.

B. *Stochastic image segmentation*

In this work, parameters used for segmentation in (15) are chosen as: $\mu_1=\mu_2=1$, $\lambda_1=\lambda_2=1$, and time-step $\Delta t=0.1$. Fig. 4 shows three different case scenarios. Results obtained with the *stochastic segmentation* (green line) are compared to the *deterministic method* (red line).

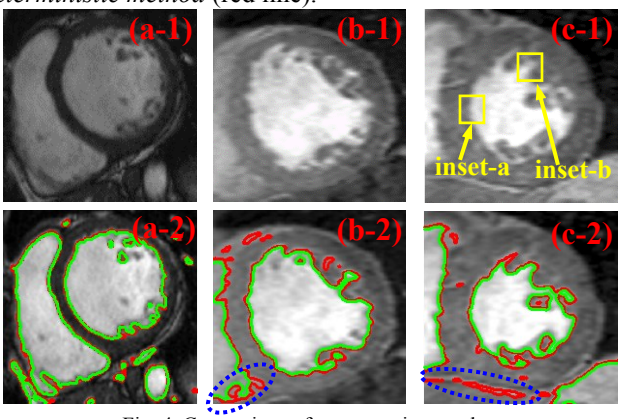

Fig. 4. Comparison of segmentation results

To illustrate the efficiency, the stochastic segmentation is applied to an image as shown in Fig. 4 a-1. The contrast of pixel values between cardiac chambers and background is very high, which results in a clear boundary. Results obtained with both methods are in a good agreement. For a second case study, both algorithms are applied to an image that has blurry boundaries resulting from such as non-compact myocardium as shown in Fig. 4 b-1. The cardiac regions can be properly detected in Fig. 4 b-2. However, boundaries obtained with the stochastic algorithm is slightly different from the deterministic method. This is because the variability in the pixel values along and on the boundaries can contribute to the optimization in (15) due to the calibration step in (16). To minimize the cost, the last two terms will penalize the regularity of boundary and enclosed area, which results in a better segmentation. This effect is farther confirmed in a third case study, where the gPC model of pixel values is applied to an image in Fig. 4 c-1, instead of the neighborhood. The gPC model in this case study is calibrated with neighborhoods of all cardiac chambers. Compared to the deterministic method, the stochastic method provides a better segmentation because of model calibration. For example, the stochastic method can eliminate artifacts that are not cardiac chambers as seen in Fig. 4 c-2. It should be noted that only the mean of a zero level set function Z is shown in the above-mentioned case studies for brevity. As discussed in Section II, the higher order gPC coefficients in (10) can provide a probabilistic measure of segmentation. This is very useful to evaluate the confidence interval along the boundary of segmentation. For example, the average of variances calculated with the higher order gPC coefficients of Z for two insets in Fig. 4 c-1 are 0.03 and 0.1, respectively. This provides segmentation variability along the boundary, and can be refereed to the PDF profiles estimated with (10) to evaluate the segmentation reliability.

IV. CONCLUSIONS

In this work, an automated stochastic image segmentation algorithm is developed to segment cardiac chambers from the background of CMR images. A generalized polynomial chaos (gPC) expansion is combined with a level set function to evolve the boundary in a stochastic way. The current design takes into account uncertainty in pixel values, quantifies and propagates it onto image segmentation steps. The method here does not require prior information of the heart, since the gPC model calibration is based on a pre-processing procedure, i.e., *deterministic segmentation* and an extension method to build an immediate neighborhood in each image. Using pixel values inside the neighborhood, the gPC model calibration can be applied to cardiac chambers. The probabilistic descriptions of heart boundary enable reliable and robust segmentation.

References

[1] C. Petitjean and J.-N. Dacher, "A review of segmentation methods in short axis cardiac MR images," *Medical Image Anlysis,* vol. 2, no. 169-184, p. 15, 2011.

[2] D. Mahapatra, "Cardiac image segmentation from cine cardiac MRI using graph cuts and shape priors," *Journal of Digital Imaing,* vol. 26, pp. 721-730, 2013.

[3] T. F. Chan and J. Shen, Image processing and analysis variational, PDE, Wavelet, and stochastic methods, Philadelphia, PA: The Society for Industrial and Applied Mathematics, 2005.

[4] T. Preusser, H. Scharr, K. Krajsek and R. M. Kirby, "Building blocks for computer vision with stochastic partial differential equations," *International Journal of Computer Vision,* vol. 80, no. 3, pp. 375-405, 2008.

[5] T. Patz and T. Preusser, "Segmentation of stochastic images using level set propagation with uncertain speed," *Journal of Mathematical Imaging and Vision,* vol. 48, no. 3, pp. 467-487, 2014.

[6] Y. Du, H. Budman and T. Duever, "Classification of normal and apoptotic cells from fluorescence microscopy images using generalized polynomial chaos and level set function," *Microscopy and Microanalysis,* vol. 22, no. 3, pp. 475-486, 2016.

[7] D. Xiu, Numerical methods for stochastic computations: a spectral method approach, Princeton, New Jersey: Princeton University Press, 2010.

[8] T. F. Chan and L. A. Vese, "Active contours without edges," *IEEE Transactions on Image Proceessing,* vol. 10, no. 2, pp. 266-277, 2001.

[9] P. Getreuer, "Chan-Vese segmentation," *Image processing online,* vol. 2, pp. 214-224, 2012.

[10] C. Li, C.-Y. Kao, J. C. Gore and Z. Ding, "Minimization of region scalable fitting energy for image segmentation," *IEEE Transactions on Image Processing,* vol. 17, no. 10, pp. 1940-1949, 2008.

[11] Y. Du, T. A. Duever and H. Budman, "Fault detection and diagnosis with parametric uncertainty using generalized polynomial chaos," *Computers and Chemical Engineering,* vol. 76, pp. 63-75, 2015.

[12] Y. Du, H. Budman and T. Duever, "Parameter estimation for an inverse nonlinear stochastic problem: reactivity ratio studies in copolymerization," *Macromolecular Theory and Simulations,* vol. 26, no. 2, p. 1~14, 2017.